

## Critical properties of the Ising model on Sierpinski fractals: A finite-size scaling-analysis approach

José M. Carmona\*

*Departamento de Física Teórica, Universidad de Zaragoza, Plaza S. Francisco s/n, 50009 Zaragoza, Spain*

Umberto Marini Bettolo Marconi†

*Dipartimento di Matematica e Fisica and Istituto Nazionale di Fisica della Materia, Università di Camerino,  
Via Madonna delle Carceri, 62032, Camerino, Italy*

Juan J. Ruiz-Lorenzo‡

*Dipartimento di Fisica and Istituto Nazionale di Fisica Nucleare (Sez. Roma-I), Università di Roma La Sapienza, P. A. Moro 2,  
00185 Roma, Italy*

Alfonso Tarancón§

*Departamento de Física Teórica, Universidad de Zaragoza, Plaza S. Francisco s/n, 50009 Zaragoza, Spain*

(Received 2 February 1998; revised manuscript received 9 July 1998)

The present paper focuses on the order-disorder transition of an Ising model on a self-similar lattice. We present a detailed numerical study, based on the Monte Carlo method in conjunction with the finite-size scaling method, of the critical properties of the Ising model on some two-dimensional deterministic fractal lattices with different Hausdorff dimensions. Those with finite ramification order do not display ordered phases at any finite temperature, whereas the lattices with infinite connectivity show genuine critical behavior. In particular, we considered two Sierpinski carpets constructed using different generators and characterized by Hausdorff dimensions  $d_H = \ln 8 / \ln 3 = 1.8927 \dots$  and  $d_H = \ln 12 / \ln 4 = 1.7924 \dots$ , respectively. The data show in a clear way the existence of an order-disorder transition at finite temperature in both Sierpinski carpets. By performing several Monte Carlo simulations at different temperatures and on lattices of increasing size in conjunction with a finite-size scaling analysis, we were able to determine numerically the critical exponents in each case and to provide an estimate of their errors. Finally, we considered the hyperscaling relation and found indications that it holds, if one assumes that the relevant dimension in this case is the Hausdorff dimension of the lattice. [S0163-1829(98)02545-4]

### I. INTRODUCTION

The present understanding of phase transitions has greatly benefited from the study of the spin-lattice models, perhaps the simplest examples of extended systems showing non-trivial cooperative behavior, such as spontaneous symmetry breaking. In most cases one is interested in studying systems whose geometrical properties are regular so that one assumes that the spins occupy the cells of a regular Bravais lattice. Near the critical point, i.e. when the correlation length is much larger than the lattice spacing, the influence of the lattice structure becomes negligible and only the embedding dimension, the number of components of the order parameter together with its symmetry, and the nature of the couplings concur to determine the values of the critical exponents.

Such universal behavior is absent if the lattice is a fractal, because the translational invariance is replaced by the much weaker dilation invariance. Notwithstanding the intense activity on various physical problems in a space which instead of being Euclidean is a fractal lattice, the issue of the phase transitions and of the critical properties on self-similar supports has been rarely addressed.<sup>1-3</sup> Unlike critical phenomena in spaces of integer dimension those occurring in self-similar geometries have not been explored so far, apart from some isolated cases. One expects that the lack of transla-

tional invariance plays a crucial role in phase transitions on fractal supports. These systems besides serving in practice to model natural materials such as porous rocks, aerogels, sponges, etc., provide a geometric realization of noninteger Hausdorff dimension. Therefore they offer a possibility of testing the  $\epsilon$ -expansion technique for  $\epsilon$  not integer. Finally, one can explore systems whose geometrical dimension is very near to its lower critical dimension (in the Ising model is one: i.e., one is the larger (integer) dimension in which the system does not have a phase transition at finite temperature).

In the present study we shall consider lattices obtained by removing sites from a square lattice. If the diluted lattice is generated by a sequence of random deletions one obtains the so-called site diluted Ising model (SDIM), whose phase diagram has been studied (see, for instance, Refs. 4-6). In this case, one finds that the critical temperature  $T_c$  tends to zero as the probability  $p$  of having a site tends to the percolation threshold  $p_c = 0.592746$  (on a square lattice). Notice that only at the percolation threshold  $p_c$  the lattice manifests true self-similarity [and fractal dimension 1.8958 (Ref. 7)], but the phase transition occurs only at  $T=0$ . Thus to observe simultaneously genuine criticality and self-similarity we consider a nonstochastic lattice, the so-called Sierpinski carpet (SC). As pointed out some years ago, one can decide

whether a lattice is able to support an order-disorder transition of the Ising type by looking at its order of ramification  $\mathcal{R}$ , which is finite if after eliminating a finite number of bonds one can isolate an arbitrarily large sublattice. Only if  $\mathcal{R}=\infty$  does a phase transition occur. Thus the SC displays a critical point at finite temperature, while the Sierpinski gasket does not, being characterized by a finite  $\mathcal{R}$ . This is a manifestation of the fact that, when considering nonregular structures, the embedding dimension alone is not sufficient to determine the phase behavior.

The deterministic SC we consider, in spite of having a lower Hausdorff dimension than that of the SDIM, is always above the percolation threshold by construction. One can thus observe the interplay between fractal geometry and thermodynamics.

In the present work we shall investigate the critical behavior of the Ising model on two classes of fractal lattices, the two-dimensional Sierpinski gasket and the two-dimensional Sierpinski carpet. The first lattice, with Hausdorff dimension  $d_H=\ln 15/\ln 5=1.682\ 606\dots$ , can be studied analytically and an exact real-space renormalization-group treatment rules out the possibility of a finite ordering temperature. The Sierpinski carpet instead displays a genuine transition at finite temperature that we have characterized numerically for two different fractal dimensions,  $d_H=\ln 8/\ln 3$ , and  $d_H=\ln 12/\ln 4$ .

In statistical mechanics it is usually assumed that in the infinite volume limit ( $V\rightarrow\infty$ ) the average of a given observable calculated over a subvolume sufficiently large compared with the bulk correlation length yields a result independent of the particular choice and location of the cell within the sample, and moreover, that this average converges to the average value over the whole sample. In the fractal lattices that we consider such a property breaks down below the critical point because the system cannot be regarded as a uniform material over length scales larger than the correlation length, due to the presence of voids of all sizes which render the system effectively not uniform. Even the correlation length depends on the position. However we shall show that this system has a second-order phase transition and that means the existence of a divergent length scale  $\xi_\infty$  in the thermodynamic limit. Although the fractal is not homogeneous, we postulate the existence of this ‘‘average’’ correlation length at least near criticality. To assume the existence of such a length is in some sense similar to what happens when studying the diffusion problem on a lattice. There, of course, a walker does not diffuse with the same law from any point of the lattice, but one can still define a diffusive type of behavior of the type  $R\sim t^{1/d_w}$  by averaging over all possible initial positions of the walker.

We outline the plan of the paper: in Sec. II we introduce the lattices and define the observables of the Ising model which will be measured in the simulations, and give some details about the numerical procedure employed to obtain the statistical averages. In Sec. III we illustrate some analytical results concerning lattices with finite ramification order, which were obtained by means of an exact Migdal-Kadanoff decimation procedure. In Sec. IV we recall briefly the statement of the finite size scaling method. In Sec. V we illustrate the results of the simulations for the fractal characterized by  $d_H=\ln 8/\ln 3$  and discuss at some length the details of the

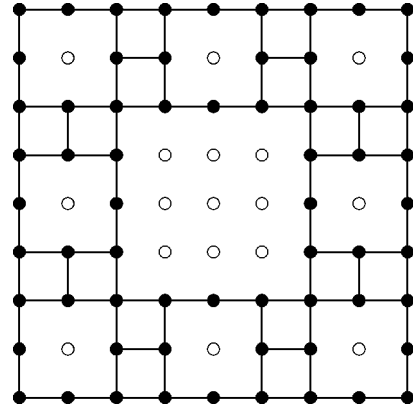


FIG. 1. SC of dimension  $d_H=\ln 8/\ln 3$  for  $L=9$ . Filled circles represent cells to which Ising spins are assigned, whereas empty circles represent cells which have been eliminated from the original square lattice. The links represent the interactions among spins.

data analysis on the basis of which we determined the values of the various critical exponents and of the critical coupling. In Sec. VI we illustrate the results of the simulations for the fractal with  $d_H=\ln 12/\ln 4$ , with special emphasis on the hyperscaling relation. Finally in Sec. VII we present the conclusions.

## II. THE MODEL AND OBSERVABLES

Let us introduce the lattice models that we shall consider in numerical studies. We have first considered a SC, named hereafter fractal *A*, constructed starting from a square lattice of  $L\times L$  cells with  $L=3^n$ , dividing it into  $3\times 3$  blocks of equal size and discarding the cells contained in the central block. Divide again each of the remaining blocks into  $3\times 3$  sub-blocks and discard all the central elements. Carry on this procedure until the smallest sub-block contains a single cell. The resulting structure is formed by  $V$  cells, where  $V$  is related to the linear dimension through the Hausdorff dimension  $d_H$  as  $V=L^{d_H}$ . In this case,  $d_H=\ln 8/\ln 3=1.892\ 789\dots$ . Of course one can build many different SC with the same fractal dimension, but having different distributions of voids. This can be quantified by means of the so-called lacunarity.<sup>8</sup> In the present work we stick to the symmetrical fractal shown in Fig. 1. We define bonds between the remaining cells. The number of bonds  $N$  is

$$N=\frac{8}{5}V+\frac{2}{5}L, \quad (1)$$

so that  $N$  is proportional to  $V$  in the thermodynamic limit. Note that this fractal has  $\mathcal{R}=\infty$ .

For the fractal *B*, the construction follows the same procedure, but now one considers  $4\times 4$  blocks and discards the four central ones. This lattice has fractal dimension  $d_H=\ln 12/\ln 3=1.792\ 481\dots$  and in this case the relation between the number of bonds  $N$ , the linear dimension  $L$ , and the number of cells  $V$  is

$$N=\frac{3}{2}V+\frac{1}{2}L. \quad (2)$$

Now, at each unit cell we assign a dichotomic spin variable  $\sigma = \pm 1$ . The total energy of the system with ferromagnetic interactions is defined as

$$\mathcal{H} = - \sum_{\langle i,j \rangle} \sigma_i \sigma_j, \quad (3)$$

where  $\langle i,j \rangle$  are nearest-neighbor cells. The energy normalized to the number of links is a quantity that has a well-defined thermodynamic limit, and the specific heat is

$$C = N(\langle E^2 \rangle - \langle E \rangle^2). \quad (4)$$

Since our primary target is to obtain information about the critical behavior of the model we first locate the critical point and then we extract the critical exponents. To achieve this goal we introduce the observables which are relevant. These are defined as follows: the intensive magnetization  $M$

$$M = \frac{1}{V} \sum_i \sigma_i, \quad (5)$$

the isothermal susceptibility:

$$\chi = V(\langle M^2 \rangle - \langle M \rangle^2), \quad (6)$$

and the Binder cumulant

$$U = \frac{1}{2} \left( 3 - \frac{\langle M^4 \rangle}{\langle M^2 \rangle^2} \right). \quad (7)$$

### III. MIGDAL-KADANOFF METHOD

The Migdal-Kadanoff (MK) decimation is an approximation very suitable for analyzing low dimensional systems. MK is exact in one dimension, but lacks predictability in higher dimensions. The starting point is the formula for the variation of the inverse temperature ( $\beta$ ) with the scale factor in the MK approximation in a system of dimensionality  $D$ ,<sup>9,10</sup>

$$\frac{d\beta}{dt} = g(\beta), \quad (8)$$

$$g(\beta) = (D-1)\beta + \sinh(\beta) \cosh(\beta) \ln[\tanh(\beta)], \quad (9)$$

where  $t$  is the logarithm of the scale factor in the block construction.

The zeroes of  $g(\beta)$  yield the inverse critical temperatures of the system. Also, it is possible to compute the  $\nu$  exponent from

$$\frac{1}{\nu} = \left. \frac{dg(\beta)}{d\beta} \right|_{\beta=\beta_c}. \quad (10)$$

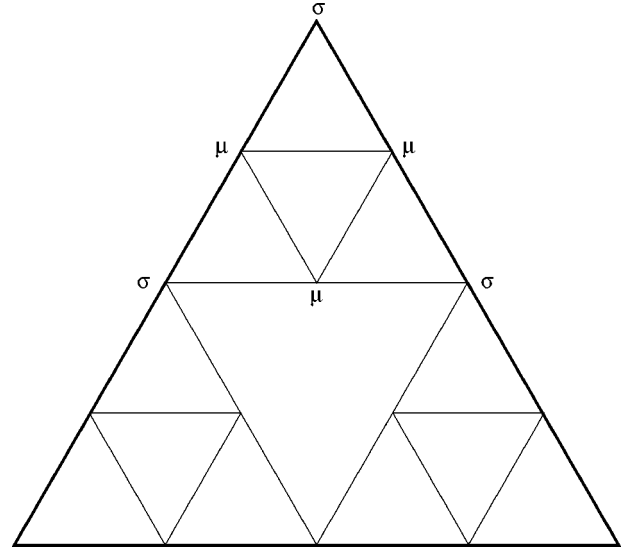


FIG. 2. Sierpinski gasket (SG). The spins live in the sites of the construction. We have marked with  $\mu$  the spins that are decimated. See the text for more details.

Such a formula is very interesting because one can obtain the behavior of the critical exponents and the critical temperature near the lower critical dimension of the Ising model; for instance when  $D \rightarrow 1$

$$\beta_c \approx \frac{1}{2(D-1)}, \quad \nu \approx \frac{1}{D-1}. \quad (11)$$

If one assumes that the dimensionality of the system corresponds to the Hausdorff dimension (i.e.  $D = d_H = 1.892789\dots$ ) one obtains  $\beta_c \approx 0.56$  and  $\nu \approx 1.12$ . Numerically [solving  $g(\beta_c) = 0$  and  $1/\nu = g'(\beta_c)$  for  $D = 1.89$ , that corresponds to fractal  $A$ ] one obtains

$$\beta_c = 0.5120, \quad \nu = 1.409. \quad (12)$$

For the fractal  $B$  ( $D = 1.79$ ) the results are

$$\beta_c = 0.5906, \quad \nu = 1.511. \quad (13)$$

Obviously this approach does not take into account the ramification and lacunarity of the model. Nonetheless in this section we have obtained a first guess of the critical temperature and of the  $\nu$  exponent for a system with the same fractal dimension that the Sierpinski carpet (in the most symmetric version) that we will study numerically in the next sections.

#### Exact solution of the Sierpinski gasket

The decimation can be carried out exactly on the Sierpinski gasket, recovering the same lattice after a decimation transformation.

We express the Boltzmann weight in the usual way

$$\exp(\beta s_1 s_2) = \cosh(\beta) [1 + s_1 s_2 \tanh(\beta)], \quad (14)$$

where we have denoted by  $s_1$  and  $s_2$  two generic spins belonging to the lattice. We denote by  $\mu$  the spins that we decimate and by  $\sigma$  the rest of the spins.

The decimation over the  $\mu$  spins is the following (see Fig. 2).

$$\begin{aligned}
& \sum_{\mu_1, \mu_2, \mu_3 = \pm 1} \exp[\beta(\sigma_1\mu_1 + \sigma_1\mu_2 + \mu_1\mu_2 + \mu_1\sigma_2 + \mu_1\mu_3 + \mu_2\mu_3 + \mu_2\sigma_3 + \mu_3\sigma_3 + \mu_3\sigma_2)] \\
&= F \sum (1+k\sigma_1\mu_1)(1+k\sigma_1\mu_2)(1+k\mu_1\mu_2)(1+k\mu_1\sigma_2)(1+k\mu_1\mu_3) \\
&\quad \times (1+k\mu_2\mu_3)(1+k\mu_2\sigma_3)(1+k\mu_3\sigma_3)(1+k\mu_3\sigma_2) \\
&= 8(1+k)^3(1+k^2)(1-3k+5k^2-3k^3+k^4) \left[ 1 + \frac{k^2}{1-3k+5k^2-3k^3+k^4} (\sigma_1\sigma_2 + \sigma_1\sigma_3 + \sigma_2\sigma_3) \right], \tag{15}
\end{aligned}$$

where we have defined  $k \equiv \tanh(\beta)$  and  $F = \cosh^9(\beta)$ .

The Sierpinski gasket is self-similar under this decimation transformation and we can see that Eq. (15) corresponds to a nearest-neighbor Ising interaction with a renormalized coupling ( $\beta_R$ ). i.e.,

$$\begin{aligned}
& \exp[\beta_R(\sigma_1\sigma_2 + \sigma_2\sigma_3 + \sigma_3\sigma_1)] \\
&= F'(1+k_R\sigma_1\sigma_2)(1+k_R\sigma_1\sigma_3)(1+k_R\sigma_2\sigma_3) \\
&= F'(1+k_R^3) \left[ 1 + \frac{k_R(1+k_R)}{1+k_R^3} (\sigma_1\sigma_2 + \sigma_1\sigma_3 + \sigma_2\sigma_3) \right], \tag{16}
\end{aligned}$$

and we have denoted with  $k_R = \tanh(\beta_R)$  the renormalized  $k$  and  $F' = \cosh^3(\beta_R)$ . We finally arrive at the following exact recursion [by matching the coefficient of  $(\sigma_1\sigma_2 + \sigma_2\sigma_3 + \sigma_3\sigma_1)$  of Eqs. (15) and (16)]

$$\frac{k^2}{1-3k+5k^2-3k^3+k^4} = \frac{k_R(1+k_R)}{1+k_R^3}. \tag{17}$$

The critical points correspond to the solutions of the previous recursion formula. The solutions are  $k=0$  and  $k=1$ , i.e., are  $\beta=0$  and  $\beta=\infty$ : there is no phase transition at any finite temperature. From Fig. 2 it is clear that  $\mathcal{R}$  remains finite even when the linear size diverges.

#### IV. FINITE-SIZE SCALING METHOD (FSS)

For a finite system whose typical linear size is  $L$ , which is assumed to be much larger than the lattice spacing  $a$ , the finite-size scaling hypothesis<sup>11,12</sup> postulates that upon approaching the critical point the average value of a given observable  $P$  depends on the size and on the temperature through the following scaling relation:

$$\frac{P_L(t)}{P_\infty(t)} = f\left(\frac{L}{\xi_\infty(t)}\right), \tag{18}$$

where  $T_c$  and  $t$  are, respectively, the critical and the reduced temperature  $t = |T - T_c|/T_c$  of the system, and  $P_\infty$  represents the value of  $P$  in the infinite volume limit. If  $P_\infty(t)$  behaves as  $t^{-\rho}$  when  $t \rightarrow 0$ , since the correlation length diverges as  $\xi_\infty \sim t^{-\nu}$ , it is clear that  $P_L(t)$  will saturate when the  $\xi_\infty$  becomes comparable with  $L$ . This can be formalized by writing:

$$P_L(t) = L^{\rho/\nu} g(tL^{1/\nu}), \tag{19}$$

where the scaling function  $g(x)$  has the limiting behavior  $g(x) = \text{const}$  as  $x \rightarrow 0$  and  $g \sim x^{-\rho}$  as  $x \rightarrow \infty$ .

Thus at the critical point one can write the following finite-size scaling formulas for the observables (see, for instance, Ref. 5):

$$\chi(L, t=0) \propto L^{\gamma/\nu} [1 + O(L^{-\omega})], \tag{20}$$

$$C(L, t=0) \propto L^{\alpha/\nu} [1 + O(L^{-\omega})], \tag{21}$$

where  $\omega$  is the correction-to-scaling exponent (it is just the slope of the field-theoretical  $\beta$  function at the fixed point or equivalently the largest irrelevant scaling exponent in the Wilson renormalization group), and  $t$  is the reduced temperature of the model.

For nondimensional quantities, denoted by  $A$ , in the proximity of the critical point ( $t \ll 1$ ) one has the scalings:

$$A(L, t) = f_A(L^{1/\nu}t) + L^{-\omega} g_A(L^{1/\nu}t) + O(L^{-2\omega}), \tag{22}$$

where  $f_A$  and  $g_A$  are scaling functions. Their derivatives with respect to  $\beta$  behave as

$$\frac{dA}{d\beta}(L, t=0) \propto L^{1/\nu} [1 + O(L^{-\omega})]. \tag{23}$$

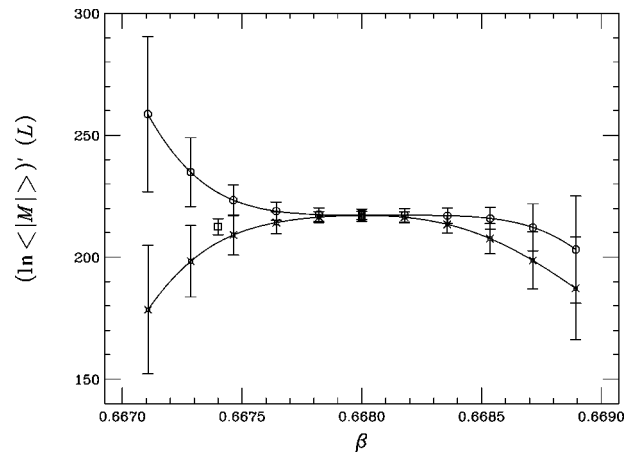


FIG. 3. SDM extrapolation for the derivative of  $\ln\langle|M|\rangle$  in a  $L = 2187$  lattice. Circles are results relative to Wolff algorithm, crosses are relative to SW. The extra point refers to another simulation (not a SDM extrapolation). The region where the SDM extrapolation has small errors is very small.

TABLE I. Values of the coupling  $\beta$  where the Binder cumulants meet each other.

	81	243	729	2187
27	0.6693(3)	0.67176(5)	0.67345(3)	0.67455(2)
81		0.6730(2)	0.67422(5)	0.67502(1)
243			0.67486(7)	0.67546(4)
729				0.6759(1)

In particular in the present work we have chosen  $A$  to be the Binder cumulant  $U$  and  $A = \ln\langle|M|\rangle$ .

The  $\omega$  exponent can be calculated using the effective critical exponents that are extracted from the peaks of the observables at lattice sizes  $L$  and  $sL$ . Let us take the susceptibility, for example. We obtain the effective  $(\gamma/\nu)(L, sL)$  as

$$\frac{\gamma}{\nu}(L, sL) = \frac{1}{\ln s} \ln \frac{\chi(sL)}{\chi(L)}. \quad (24)$$

Using the scaling formulas and working in the large lattices, we obtain

$$\frac{\gamma}{\nu}(L, sL) = \frac{\gamma}{\nu} + BL^{-\omega}, \quad (25)$$

where  $\gamma/\nu$  is the infinite volume extrapolation of the ratio  $\gamma/\nu(L, sL)$  measured on finite lattices. We obtain  $\omega$  and  $\gamma/\nu$  by fitting the data to formula (25).

In order to determine the critical temperature, let us call  $\beta_c^O(L)$  the value of  $\beta$  where the observable  $O$  (with positive dimension) displays a maximum. In order to assess its location several simulations at different values of  $\beta$  are needed in principle, and even doing so its precise determination is hard. However, the spectral density method<sup>13</sup> (SDM) renders such task easier and much faster. In fact, by using the data from a single simulation at a given temperature, say  $\beta_0$ , one can obtain information about some  $\beta_1$  in the neighborhood of  $\beta_0$ . With SDM one usually gains one order of magnitude in the accuracy of the location of the peak.

The idea is to write the partition function under the form:

$$\begin{aligned} Z &\propto \sum_{\{\text{confs}\}} e^{-\beta\mathcal{H}(\sigma)} = \sum_E \sum_{\{\text{confs}\}} e^{-\beta\mathcal{H}(\sigma)} \delta(\mathcal{H} - E) \\ &= \sum_E e^{-\beta E} N(E), \end{aligned} \quad (26)$$

where  $\mathcal{H}(\sigma)$  is the Hamiltonian as a function of the configuration  $\{\sigma\}$  and  $N(E)$  is the energy density of states, which

TABLE II. Maxima of  $(\ln\langle|M|\rangle)'(L)$ .

$L$	No. files	$\beta_{\text{sim}}$	$\beta_O(L)$	Max. of $(\ln\langle M \rangle)'(L)$
27	~ 6600	0.580	0.5796(3)	13.19(1)
81	~ 5800	0.629	0.6275(1)	28.46(6)
243	~ 4000	0.650	0.6505(2)	58.5(2)
729	~ 13900	0.6618	0.6622(1)	115.4(4)
2187	~ 6400	0.6682	0.6681(2)	218(1)

TABLE III. Maxima of  $U'(L)$ .

$L$	No. files	$\beta_{\text{sim}}$	$\beta_O(L)$	Max. of $U'(L)$
27	~ 6600	0.580	0.5744(3)	8.40(2)
81	~ 5800	0.629	0.6252(2)	17.56(9)
243	~ 4000	0.650	0.6493(2)	35.8(2)
729	~ 13900	0.6618	0.6617(1)	69.8(4)
2187	~ 2400	0.668	0.6680(3)	132(3)

can be obtained from the number of times that the value  $E$  of the energy is generated during a Monte Carlo (MC) simulation. Given the density of states at  $\beta = \beta_0$ , the value of a certain operator  $O$  at  $\beta_1 \neq \beta_0$  is given by

$$\langle O(\beta_1) \rangle = \frac{\sum_E O(\beta_0, E) N(E) e^{-(\beta_1 - \beta_0)E}}{\sum_E N(E) e^{-(\beta_1 - \beta_0)E}}. \quad (27)$$

This extrapolation is exact. The problem is that for large deviations  $\Delta\beta = \beta_1 - \beta_0$  the errors in the extrapolation are very large, and then one has to restrict oneself to small  $\Delta\beta$  values (of order  $1/\sqrt{V}$ ).

In  $d \geq 2$  the value  $\beta_c^O(L)$  hardly changes with  $O$ , and with the help of the SDM one can reach the peak of every observable with a single simulation at a certain  $\beta$ . We found that this is not the case on fractal lattices with  $d_H < 2$  because the transition region turns out to be very large, and sometimes we were forced to perform different simulations at different points, depending on the observables, in order to get their corresponding peaks.

To compute thermal averages we have employed a combination of  $m$  steps of the classical Metropolis algorithm followed by  $n$  steps of the Wolff single-cluster algorithm,<sup>14</sup> which gives a very short autocorrelation time. We checked that such method is sufficient to ensure ergodicity. However, the Wolff algorithm is unable to flip clusters of intermediate size, which might be important in our model, where there are domains of spins at every scale. That is why we have applied in addition a Swendsen-Wang (SW) algorithm,<sup>15</sup> which is more consuming in computing time than the Wolff algorithm, but is able to flip domains of spins of every scale. In fact, we have compared the results of the two different procedures. Figure 3 shows that the two methods give compatible results in a region around the simulation point, where the SDM extrapolation is valid (away from this region, the SDM extrapolation gives large errors and it is therefore not reliable, so that it is not surprising that it gives different results for the two algorithms). We also note the narrow range of

TABLE IV. Maxima of  $\chi(L)$ .

$L$	No. files	$\beta_{\text{sim}}$	$\beta_\chi(L)$	Max. of $\chi(L)$
27	~ 6600	0.580	0.59431(6)	27.97(3)
81	~ 5800	0.629	0.63442(4)	179.2(2)
243	~ 2000	0.651	0.65394(7)	1164(4)
729	~ 8000	0.663	0.66402(2)	7759(7)
2187	~ 4400	0.669	0.66936(1)	51883(58)

TABLE V. Fits to Eq. (28) for different observables  $O$ , lattices 81, 243, 729, and 2187.

$O$	$\beta_c(\infty)$	$\nu^{-1}$
$\chi$	0.67522(7)	0.589(3)
$(\ln\langle M \rangle)'$	0.6742(5)	0.62(1)
$U'$	0.6747(7)	0.61(2)

validity of the SDM which is used to extrapolate the numerical data, which makes even more troublesome the problem of finding the peaks of observables in order to perform FSS. As far as the observables directly measured are concerned one can hardly see differences in the two simulation algorithms; however, discrepancies exist when one looks at the derivatives of the measured quantities.

## V. NUMERICAL RESULTS FOR THE FRACTAL A

We now focus attention on the SC of fractal dimension  $d_H = \ln 8 / \ln 3$  described in Sec. II (fractal A), and provide evidence of the existence of a phase transition at a finite value of  $\beta$ . The behavior of the SC should interpolate between the  $d=1$  and  $d=2$  cases. In  $d=1$ ,  $\beta_c$  diverges. In fact, with a similar analysis of the partition function to the one used in the Appendix, it can be analytically calculated that  $\xi(\beta) \sim |\ln \tanh(\beta)|^{-1}$ , which means that, when  $\beta \rightarrow \infty$ ,  $\xi(\beta) \sim e^{2\beta}$ . If we define  $\beta_c(L)$  as the value of  $\beta$  for which  $\xi \approx L$ , then  $\beta_c(L) \sim \ln L$  in  $d=1$ . This means a smooth growth; it is therefore necessary to pay attention in order to demonstrate that  $\beta_c(L)$  does not diverge with  $L$  in the case under scrutiny.

We performed different simulations for lattice sizes with  $L=27, 81, 243, 729$ , and 2187, and concluded that there are several evidences of the occurrence of a phase transition in the Ising model on this Sierpinski carpet. Not only the average magnetization changes from 0 to 1 going from the disordered to the ordered phase, but we also observed that some observables, shown below, present peaks increasing as powers of the size,  $L$ . The most stringent criterion to locate the critical coupling,  $\beta_c$  is to study the crossing of the Binder cumulants relative to different volumes. In  $d=1$ , where there is not a phase transition at a finite value of  $\beta$ , the cumulants cross each other at  $\beta = \infty$ . This is not the case in this model.

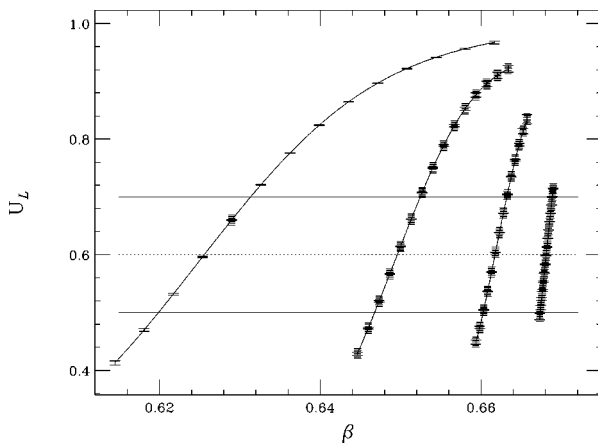


FIG. 4. Binder cumulants for  $L=81, 243, 729, 2187$ .

TABLE VI. Values of  $\beta(L)$  where the Binder cumulants take the values 0.5, 0.6, and 0.7.

$g_0$	$L=81$	$L=243$	$L=729$	$L=2187$
0.5	0.61972(7)	0.64677(4)	0.66026(2)	0.66736(3)
0.6	0.62551(4)	0.64959(2)	0.661737(6)	0.668099(4)
0.7	0.63134(2)	0.65245(2)	0.663205(9)	0.668868(6)

The positions of the intersections of the Binder cumulants are reported in Table I and indicate that  $\beta_c \approx 0.675$ . However, considering that the curves of the largest lattices have almost the shape of a ‘‘step function,’’ and that the intersections take place within the zone of sudden change of slope, it is difficult to obtain them with good precision. We have estimated the value of  $\beta_c$  by other means, as we shall see in the next section.

It has been observed<sup>16</sup> that on fractal lattices, as the ones we consider, a certain number of stages of construction of the SC is necessary in order to obtain reliable predictions about the critical behavior. Actually, as we shall see in the next sections, we were forced to discard the smallest lattice sizes,  $L=27, 81$ , in certain fits to obtain reliable results.

### A. $\nu$ exponent and $\beta_c(\infty)$

#### 1. Position of the maxima

In a FSS analysis, every observable  $O$  which diverges in the thermodynamic limit when  $\beta = \beta_c(\infty)$  displays a peak for finite  $L$ , located at a different value  $\beta_O(L)$ . When  $L$  increases, the difference between  $\beta_O(L)$  and  $\beta_c(\infty)$  becomes smaller according to the law

$$\beta_O(L) - \beta_c(\infty) \propto L^{-1/\nu}. \quad (28)$$

A three-parameter fit determines the values of exponent  $\nu$  and of  $\beta_c(\infty)$ . To produce such a fit we have considered three different observables: the derivative of the logarithm of the magnetization, the derivative of the Binder cumulant (7) and the isothermal susceptibility (6). These three quantities display maxima at the values of  $\beta_O(L)$  shown in Tables II, III and IV, respectively. In these tables we report the values of the peaks for the different lattice sizes together with the statistics performed in correspondence with each  $L$ . Here and in the following, each file is made of 200 steps of SW, 400 steps of Metropolis and 2000 cluster sweeps with the Wolff algorithm. The integrated correlation time is always less than a file of measurements.

The best fits are obtained discarding the  $L=27$  data from the three tables. We obtain the results shown in Table V. All the fits yield  $\chi^2/DF < 1$  (where DF means the number of degrees of freedom in the fit); we conclude from these that

TABLE VII. Fit of the values of Table VI to Eq. (28).

$g_0$	$\beta_c(\infty)$	$\nu^{-1}$
0.5	0.6753(2)	0.585(6)
0.6	0.6751(4)	0.589(2)
0.7	0.6752(1)	0.584(3)

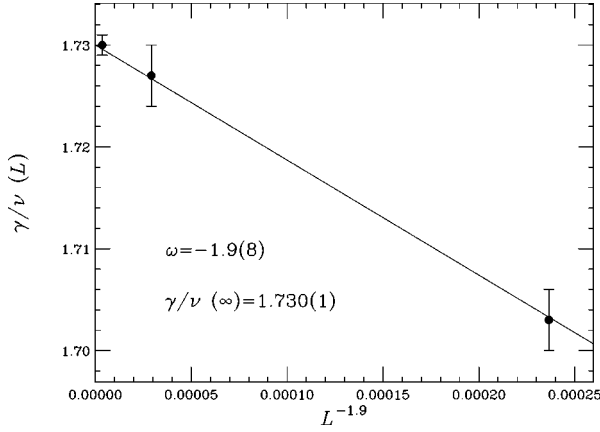


FIG. 5. Fit to obtain the scaling corrections in  $\chi$  using  $L = 81, 243, 729, 2187$ .

$$\beta_c(\infty) = 0.6751(1) \quad \nu^{-1} = 0.59(1), \quad (29)$$

and

$$\nu = 1.70(1). \quad (30)$$

We remark that we obtain a better result using the susceptibility than the other two observables (the derivatives of the logarithm of the absolute value of the magnetization and of the Binder cumulant).

### 2. Fits at fixed values of the Binder cumulant

Let us now check the values of  $\beta_c(\infty)$  and  $\nu$  obtained (see Table V) employing Eq. (28) with different definitions of the apparent critical coupling  $\beta_o(L)$ . We consider now a fixed value  $g_0$  of the Binder cumulant  $U_L(\beta)$ , and define  $\beta(L)$  via the equation

$$U_L(\beta(L)) = g_0. \quad (31)$$

It is clear from Ref. 17 that  $\beta(L)$  behaves like  $\beta_o(L)$ , see Eq. (28).

We have used for  $g_0$  the values 0.5, 0.6, and 0.7 (see Fig. 4). The values of the  $\beta(L)$  given by condition (31) are collected in Table VI for the lattice sizes  $L = 81, 243, 729, 2187$ , and the results of fitting these values to Eq. (28) are shown in Table VII. We see that these values of  $\beta_c(\infty)$  and  $\nu^{-1}$  are compatible with those given in Eq. (29). We remark that the fits reported in Table VII have been obtained using only the lattice sizes 243, 729, and 2187. In all these fits the number of degrees of freedom is zero, and the reader should take the results of Table VII as a check of our previous estimates of  $\beta_c$  and  $1/\nu$ .

### 3. Peaks of $(\ln\langle|M|\rangle)'(L)$ and $U'_L$

According to the finite-size-scaling ansatz the derivatives of  $(\ln\langle|M|\rangle)(L)$  and  $U_L$  must show a peak increasing as  $L^{1/\nu}$ . The values of the maxima in correspondence with each  $L$  are reported in Tables II and III.

In the case of  $U'_L$  a two-parameter fit gives

$$L > 81: \quad \nu^{-1} = 0.600(4), \quad \chi^2/\text{DF} = 1.37, \quad (32)$$

which again agrees with our previous result Eq. (29).

For  $(\ln\langle|M|\rangle)'(L)$  we obtain

$$L = 729, 2187: \quad \nu^{-1} = 0.579(5). \quad (33)$$

For  $L > 27$  or  $L > 81$  the fits are bad (i.e.,  $\chi^2/\text{DF}$  is large).

In these two cases (derivatives of  $U$  and  $\ln\langle|M|\rangle$ ) we have not the necessary accuracy in order to have a stable fit taking into account the scaling corrections.

### B. $\gamma/\nu$ exponent: scaling of $\chi$

The isothermal susceptibility (6) displays a peak increasing as  $L^{\gamma/\nu}$ .

By fitting the peaks with  $L^{\gamma/\nu}$  we obtain a poor  $\chi^2/\text{DF}$ ; however, after discarding the data relative to  $L = 27, 81$  we obtain a  $\chi^2/\text{DF} < 1$ . The result is

$$L > 81: \quad \gamma/\nu = 1.729(1), \quad \chi^2/\text{DF} = 0.6. \quad (34)$$

In order to include also the data relative to  $L = 27, 81$ , we considered the scaling corrections to such a fit according to Eq. (24). Applying the procedure of the fit [Eq. (24)] to the data of Table IV [i.e., we compute the effective exponent  $\gamma/\nu$  using all the lattice sizes: i.e.  $\gamma/\nu(27, 81), \gamma/\nu(81, 217), \dots$ ] we find

$$\gamma/\nu = 1.76(2), \quad \omega = 0.27(14), \quad \chi^2/\text{DF} = 7, \quad (35)$$

which is unsatisfactory. However, if we discard only the  $L = 27$  data we end up with

$$L > 27: \quad \gamma/\nu = 1.730(1), \quad \omega = 1.9(8). \quad (36)$$

In the last fit, shown in Fig. 5, we have not degrees of freedom, because we have fitted three data to Eq. (24), which contains three free parameters. However, the result for  $\gamma/\nu$  is compatible with Eq. (34) having included the  $L = 81$  data and the exponent  $\omega$  represents the correction to the scaling. It is clear that the final value of  $\gamma/\nu$  in the fit is really stable (almost) independently of the  $\omega$  value.

We conclude that

$$\omega = 1.9(8), \quad \gamma/\nu = 1.730(1). \quad (37)$$

TABLE VIII. Absolute value of the magnetization at the critical point for the different lattice sizes.

$L$	$\langle M_L \rangle(0.6751)$	$\langle M_L \rangle(0.6750)$	$\langle M_L \rangle(0.6752)$	$\langle M_L \rangle(\beta_c(\infty))$
27	0.8546(2)	0.8544(2)	0.8548(2)	0.8546(4)
81	0.7945(1)	0.7942(1)	0.7949(1)	0.7945(5)
243	0.7345(1)	0.7338(1)	0.7351(1)	0.7345(8)
729	0.6742(1)	0.6729(1)	0.6754(1)	0.6742(14)
2187	0.61338(8)	0.61110(8)	0.61561(9)	0.61336(234)

TABLE IX. Comparison between the results for the phase transition in the  $d=1$ ,  $d=2$ , and  $d=1.89$  (fractal  $A$ ) Ising models.

	$\beta_c$	$\nu$	$\gamma$	$\omega$
$d=1$	$\infty$	$\infty$	$\infty$	2
this fractal	0.6752(1)	1.70(1)	2.94 (2)	1.9(8)
$d=2$	0.44...	1	1.75	4/3

By using  $\nu=1.70(1)$  we can write down the result for the  $\gamma$  exponent

$$\gamma=2.94(2). \quad (38)$$

### C. $\beta/\nu$ exponent: scaling of $\langle|M|\rangle$

Having computed the critical value of the coupling [Eq. (29)], we can extract the  $\beta/\nu$  exponent from the scaling law:

$$\langle|M_L|\rangle(\beta_c(\infty))\propto L^{-\beta/\nu}. \quad (39)$$

We have written in Table VIII the values of  $\langle|M_L|\rangle$  in correspondence with the points 0.6751, 0.6750, and 0.6752, and the final value that we take to make the fit (that is, it takes into account the error in our final value of  $\beta_c$ ).

Only by fitting the lattice sizes with  $L\geq 243$  it is possible to obtain a ‘‘reasonable’’ fit ( $\chi^2/\text{DF}=2.4/1$ ; we have only one degree of freedom), in particular

$$\beta/\nu=0.080(1). \quad (40)$$

The quality of the data is not good for trying a fit taking into account the scaling corrections.

### D. $d_s$ and hyperscaling

Having obtained the values of  $\gamma/\nu=1.730(1)$  and  $\beta/\nu=0.080(1)$  we can consider the hyperscaling relation

$$2\frac{\beta}{\nu} + \frac{\gamma}{\nu} = d, \quad (41)$$

where  $d$  is the dimension that controls hyperscaling. In our case, we obtain  $d=1.890(2)$ , which is close to the Hausdorff dimension of the lattice under scrutiny.

Finally we remark that it is clear from the standard derivation of the hyperscaling relations that the dimension that plays a role is the Hausdorff one.

### E. $\alpha/\nu$ exponent: the specific heat

The specific heat, for positive values of  $\alpha$ , has a peak which scales with  $L^{\alpha/\nu}$ . In our case, this peak is very flat showing a plateau that goes down as the lattice size increases. This corresponds to a negative value of the exponent  $\alpha$ . Our numerical estimate is  $\alpha\approx -1.15$  (which derives from  $\nu d_H=2-\alpha$ ). Notice that such a value lies between the zero value of the two-dimensional Ising model and the infinitely negative value of the one-dimensional Ising model.

As expected the exponents for the present lattice interpolate between the corresponding values of the  $d=1$  and  $d=2$  cases as shown in Table IX. The value of the  $\omega$  exponent in  $d=1$  is calculated in the Appendix.

TABLE X. Results of the simulation of the fractal  $B$ .

$L$	$\beta_{\text{sim}}$	$\beta_c(L)$	Max. of $dM/d\beta$	Max. of $\chi(L)$
64	0.7396	0.74548(6)	5.797(3)	86.57(2)
256	0.8060	0.8094(3)	9.06(2)	839.8(5)
1024	0.8480	0.8501(6)	12.67(5)	8484(3)
4096	0.8780	0.8782(6)	16.6(6)	88808(101)

## VI. NUMERICAL RESULTS FOR THE FRACTAL $B$

In order to provide further evidence for the hyperscaling relation we considered a second fractal lattice, the Sierpinski carpet  $B$ , described in Sec. II, whose Hausdorff dimension is  $d_H=\ln 12/\ln 4$ . We carried out a finite-size scaling analysis with lattice sizes of  $L=64, 256, 1024$ , and  $4096$ . We were interested in the verification of the hyperscaling relation (41). In order to get an estimate of the critical exponents  $\gamma/\nu$  and  $\beta/\nu$  from a single simulation for every size  $L$ , we considered in this case the observables  $\chi$  and the derivative of the magnetization with respect to  $\beta$ , as it is explained in the following paragraphs. The results of the simulations are shown in Table X.

The exponent  $\gamma/\nu$  is obtained from the peak of the susceptibility. A fit with the three first lattice sizes gives the value  $\gamma/\nu=1.6530(2)$ , and the value  $\gamma/\nu=1.6755(4)$  with the three last ones. This difference means the existence of scaling corrections. We shall take as our best estimate the value

$$\gamma/\nu=1.67(2). \quad (42)$$

Differentiating the magnetization with respect to  $\beta$ , we obtain a quantity which scales as  $L^{(1-\beta)/\nu}$ . Discarding again the  $L=64$  data, we find

$$\frac{1-\beta}{\nu}=0.241(3), \quad \chi^2/\text{DF}=3.1. \quad (43)$$

The large value of  $\chi^2/\text{DF}$  again shows the existence of large scaling corrections. However, using only the data of the lattice sizes  $L=1024$  and  $L=4096$  we have found  $(1-\beta)/\nu=0.20(3)$  that is compatible in the error bars with Eq. (43).

Now we need an estimate of the  $\nu$  exponent in order to get  $\beta/\nu$  from Eq. (43). We have obtained a good fit to Eq. (28) using the positions of the peaks of the derivative of  $M$  with respect to  $\beta$ . These are shown as  $\beta_c(L)$  in Table X. In this case we are dealing with a three-parameter fit, so that we need to use the four lattice sizes for consistency. Letting  $\nu$  vary freely, we obtain the best fit for

$$\nu=3.23(8), \quad \beta_c(\infty)=0.928(3), \quad \chi^2/\text{DF}=0.95. \quad (44)$$

This fit is shown in Fig. 6. Using this result for  $\nu$  and Eq. (43), we get

$$\beta/\nu=0.069(10). \quad (45)$$

With the results (42) and (45), we obtain through the hyperscaling relation (41), the value  $d=1.81(3)$ . The error in



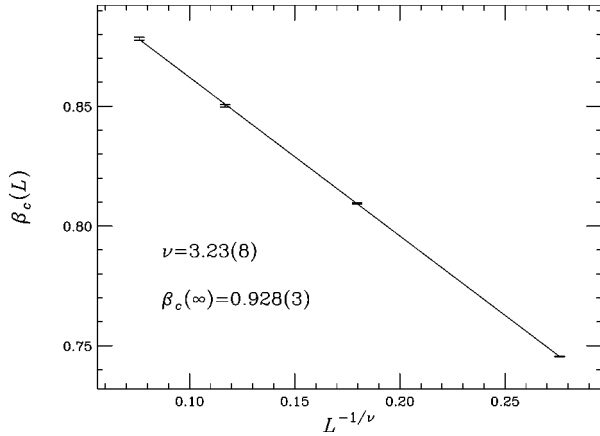


FIG. 6. Best fit to  $\beta_c(\infty)$  obtained when varying  $\nu$ , using the values of  $\beta_c(L)$  shown in Table X. The error in  $\beta_c(\infty)$  contains the uncertainty in  $\nu$ .

this value is large owing to the scaling corrections, but it is perfectly compatible with the Hausdorff dimension of the fractal.

## VII. CONCLUSIONS

In the present paper we have considered the issue of phase transitions on discrete fractal lattices. First, by means of an exact Migdal-Kadanoff decimation transformation we confirmed the absence of a finite-temperature critical point for the Sierpinski gasket.

Then we focused on lattices with infinite ramification order and performed extensive MC simulations on deterministic Sierpinski carpets of different sizes and different Hausdorff dimensions, where we observed the presence of a finite-temperature phase transition. The FSS analysis was applied in order to extract from the data the critical exponents and their numerical errors.

The present study represents a massive attempt to determine numerically the critical properties of Ising models on fractal lattices. We have illustrated the difficulties one encounters when dealing with these systems, which are due to the slow convergence of the averages to the infinite volume limit.

Interestingly, the hyperscaling relation, which was not obtained before for such lattices, indicates that the role of  $d$  of the Euclidean case is taken by the Hausdorff dimension. Finally we should comment about the universality of the present results. As pointed out by Wu and Hu,<sup>18</sup> on a true self-similar structure the statement of universality survives only in a weak version. In fact, the various exponents might depend on the detailed structure of the fractal. It has been found, by means of approximate treatments, that the exponents vary even when the fractal dimension remains fixed, because they depend also on other geometrical characteristics such as the connectivity and the lacunarity. This is not too surprising since due to the scale invariance a small change at the smallest stage may be magnified up to the largest one. In other words, the lattice structure, which in normal critical phenomena does not enter with all its details here plays a much more important role. However, we have verified that the hyperscaling relation holds for the two fractals we have considered, which suggests that for lattices hav-

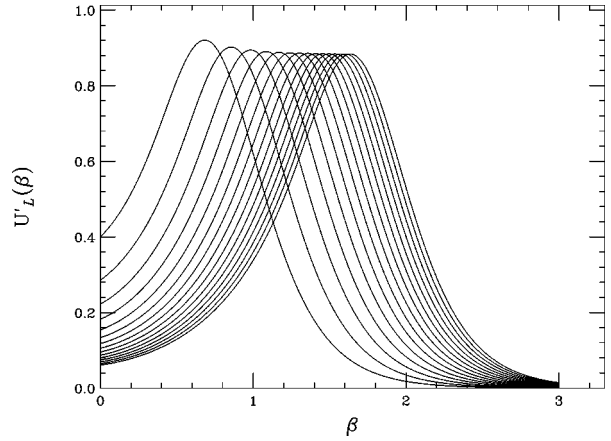


FIG. 7. Derivative of the Binder cumulant as a function of  $\beta$  for several values of  $L = 4, 8, 16, 32, 64, 128 \dots$  for the Ising model in one dimension.

ing the same fractal dimension,  $\beta$ ,  $\nu$ , and  $\gamma$  may vary with the lacunarity, but the sum of their ratios cannot. We finally remark that the model under study could provide a very good benchmark to study the thermodynamics of the Ising model near its lower critical dimension.

## ACKNOWLEDGMENTS

We wish to thank L.A. Fernández for very useful discussions. J.M.C. was supported by a Spanish MEC grant. J. J. R.-L. was supported by an EC HMC (ERBFMBICT950429) grant. The numerical work was done using the RTNN parallel machine (composed by 32 Pentium Pro processors) located at Zaragoza University.

## APPENDIX

In this appendix we will compute the correction-to-scaling exponent for the one-dimensional Ising model.

We will use the Binder cumulant (7), which can be written as

$$U_L(\beta) = - \frac{\langle M^4 \rangle_c}{2 \langle M^2 \rangle_c^2}, \quad (\text{A1})$$

where

$$\langle M^n \rangle_c = \left. \frac{\partial^n \ln \mathcal{Z}_V}{\partial h^n} \right|_{h=0}, \quad (\text{A2})$$

with  $h$  the magnetic field and  $\mathcal{Z}_V$  the partition function for the volume  $V$  (in this case,  $V \equiv L$ ).

It is possible to diagonalize exactly the transfer matrix for the one-dimensional model, and the two eigenvalues are

$$\lambda_{1,2} = e^\beta \{ \cosh(h) \pm [\sinh^2(h) + e^{-4\beta}]^{1/2} \}. \quad (\text{A3})$$

Then the partition function is

$$\mathcal{Z}_V = \lambda_1^V + \lambda_2^V. \quad (\text{A4})$$

From Eqs. (A2) and (A4), we obtain

$$\langle M^2 \rangle_c = V e^{2\beta} \frac{1 - [\tanh(\beta)]^V}{1 + [\tanh(\beta)]^V}, \quad (\text{A5})$$

and

$$\langle M^4 \rangle_c = \frac{V e^{2\beta} (3 e^{4\beta} - 1) [(2 \sinh(\beta))^{2V} - (2 \cosh(\beta))^{2V}] + 12V^2 e^{4\beta} (4 \sinh(\beta) \cosh(\beta))^V}{[(2 \sinh(\beta))^V + (2 \cosh(\beta))^V]^2}. \quad (\text{A6})$$

We put these expressions into (A1), and consider the derivative of the Binder cumulant. It has a peak at finite values of  $\beta$  for each  $L$ ,  $\beta_c(L)$ . The peak of the derivative of the Binder cumulant scales as  $L^{1/\nu}$  plus scaling corrections. In  $d=1$ ,  $\nu=\infty$ , so that we have

$$U'_L(\beta_c(L)) = A + BL^{-\omega} + O(L^{-2\omega}). \quad (\text{A7})$$

We calculated numerically this derivative and obtained the plot shown in Fig. 7 for several values of  $L$ .

Fitting to Eq. (A7) we obtain, when  $L \rightarrow \infty$ , the asymptotic limit

$$\omega = 2. \quad (\text{A8})$$

\*Electronic address: carmona@sol.unizar.es

†Electronic address: umberto.marini.bettolo@romal.infn.it

‡Electronic address: ruiz@lattice.fis.ucm.es

§Electronic address: tarancon@sol.unizar.es

<sup>1</sup> Deterministic fractal lattices and phase transitions have been studied in the past (Ref. 19), (Refs. 2,3) by different methods. In particular, (Ref. 19) used an approximate Migdal-Kadanoff bond moving renormalization-group approach and obtained results for the critical temperature of both the Sierpinski gasket and the Sierpinski carpet.

<sup>2</sup> The spherical model has been recently studied by U. Marini Bettolo Marconi and A. Petri, Phys. Rev. E **55**, 1311 (1997); J. Phys. A **30**, 1069 (1997); Philos. Mag. B **77**, 265 (1998).

<sup>3</sup> U. Marini Bettolo Marconi, Phys. Rev. E **57**, 1290 (1998).

<sup>4</sup> G. Parisi and J. J. Ruiz-Lorenzo, J. Phys. A **28**, L395 (1995).

<sup>5</sup> H. G. Ballesteros *et al.*, hep-lat/9707017 (unpublished); Nucl. Phys. B **512**, 681 (1998).

<sup>6</sup> J. J. Ruiz-Lorenzo, J. Phys. A **30**, 485 (1997); H. G. Ballesteros *et al.*, *ibid.* **30**, 8379 (1997).

<sup>7</sup> D. Stauffer and A. Aharony, *Introduction to the Percolation Theory*, 2nd ed. (Taylor and Francis, London, 1994).

<sup>8</sup> The lacunarity serves to measure the failure of a fractal to be translationally invariant. It has been found that in the Migdal-Kadanoff renormalization scheme the values of the exponents

vary not only with the fractal dimension, but also with the connectivity and lacunarity. According to Ref. 19,  $d_H$  and  $\mathcal{R}$  fixed, the exponent  $\nu$  increases with decreasing lacunarity.

<sup>9</sup> G. Martinelli and G. Parisi, Nucl. Phys. B **180**(FS), 201 (1981).

<sup>10</sup> We recall that this formula has been obtained for integer dimensions and we use its analytical prolongation to noninteger dimensions. Do not confuse this with the Migdal-Kadanoff techniques used in Ref. 19, in which the authors worked directly on the fractals.

<sup>11</sup> E. Brézin, J. Phys. (France) **43**, 15 (1982).

<sup>12</sup> M. E. Fisher and M. N. Barber, Phys. Rev. Lett. **28**, 1516 (1972).

<sup>13</sup> M. Falcioni, E. Marinari, M. L. Paciello, G. Parisi, and B. Taglienti, Phys. Lett. **108B**, 331 (1982); A. M. Ferrenberg and R. H. Swendsen, Phys. Rev. Lett. **61**, 2635 (1988).

<sup>14</sup> U. Wolff, Phys. Rev. Lett. **62**, 361 (1989).

<sup>15</sup> R. H. Swendsen and J. S. Wang, Phys. Rev. Lett. **58**, 86 (1987).

<sup>16</sup> B. Bonnier, Y. Leroyer, and C. Meyers, Phys. Rev. B **37**, 5205 (1988).

<sup>17</sup> G. Parisi and J. J. Ruiz-Lorenzo, Phys. Rev. B **54**, 3698 (1996); **55**, 6082(E) (1997).

<sup>18</sup> Y. K. Wu and B. Hu, Phys. Rev. A **35**, 1404 (1987).

<sup>19</sup> Y. Gefen, A. Aharony, and B. B. Mandelbrot, J. Phys. A **17**, 1277 (1984), and references therein.